

Majorana fermions in spin-singlet nodal superconductors with coexisting non-collinear magnetic order

Yuan-Ming Lu^{1,*} and Ziqiang Wang¹

¹*Department of Physics, Boston College, Chestnut Hill, Massachusetts 02467*

(Dated: October 15, 2019)

Different realizations of Majorana fermions in solid state materials have attracted a great deal of interests recently in connection to topological order and quantum information processing. We propose a novel way to create Majorana fermions in superconductors. We show that an incipient non-collinear magnetic order turns a spin-singlet superconductor with nodes into a topological superconductor with a stable Majorana bound state in the vortex core or on the edge. We argue that such an exotic non-Abelian phase can be realized in extended t - J models on different lattices with two explicit examples: one on the triangular lattice and the other on the square lattice. Our proposal provides a new avenue for the search of Majorana fermions in correlated electron materials where nodal superconductivity and magnetism are two common caricatures.

PACS numbers: 71.27.+a, 74.25.Ha, 74.81.Bd

A Majorana fermion is an electrically neutral fermion whose antiparticle is itself. It was proposed to exist in high-energy physics such as neutrino physics and dark matter [1]. In recent years, Majorana fermions have attracted growing attention in condensed matter physics [2–4]. Specifically, Majorana fermions can be realized as zero-energy bound states in the vortex core or on the edge of certain two-dimensional superconductors. Instead of the usual Bose or Fermi statistics, these vortices obey non-Abelian statistics [5–10] as a manifestation of topological order [11, 12]. Due to this remarkable feature, Majorana bound states (MBSs) can be utilized for topologically-protected qubits in fault-tolerant quantum computation [2, 13, 14]. Several systems have been proposed to realize MBSs, such as even-denominator fractional quantum Hall states [5, 6, 8, 15], $p + ip$ superconductors [8–10] and superfluids [16, 17], s -wave-superconductor-strong-topological-insulator interfaces [18, 19], s -wave Rashba superconductor [20–22] and spin-orbit-coupled nodal superconductors [23].

In this work, we present a novel realization of MBSs in spin-singlet superconductors with nodal excitations. We show that when a coexisting non-collinear magnetic order with a wavevector connecting two nodes of opposite momenta develops, there will be one MBS in each vortex core and on the edge of such topological superconductors. We demonstrate our proposal with two explicit examples. The first one is a nodal $d + id$ superconductor [24] coexisting with 1×3 (or 3×3) coplanar magnetic order on the triangular lattice. We argue that this state is likely to be realized in a doped t - J_2 model on the triangular lattice and is relevant for a material: superconducting sodium cobaltate $\text{Na}_x\text{CoO}_2 \cdot y\text{H}_2\text{O}$ near doping concentration $x = 1/3$ [24, 25]. The second example is a $d_{x^2-y^2}$ superconductor with coexisting $\mathbf{Q} = (Q_0, Q_0)$ coplanar magnetic order on the square lattice which may be realized in a doped t - J_1 - J_2 - J_3 model on the square lat-

tice. Experimentally the phase diagram of a wide range of strongly correlated materials, from high- T_c cuprates to heavy-fermion compounds, exhibits d -wave superconductivity [26, 27] in proximity to [28] or coexisting with [27, 29] magnetic orders. These results suggest that Majorana fermions may exist in correlated electron materials with magnetic frustration and nodal superconductivity.

We begin with a general discussion of our theory. The low-energy excitations of a nodal superconductor are massless Dirac fermions with linear dispersion around the nodes. Our basic idea is to create a topological superconductor with a single MBS in the vortex core by adding a proper mass term to the nodal fermions. Let us consider a spin-singlet superconductor with n pairs of isolated nodes located at crystal momenta $\pm \mathbf{q}_\ell$, $\ell = 1, \dots, n$. Expanding around the nodes, the low-energy BCS Hamiltonian describing the quasi-particle excitations has a generic form in the Nambu basis $\Psi_{\ell\mathbf{k}} \equiv (c_{\mathbf{q}_\ell+\mathbf{k},\uparrow}, c_{-\mathbf{q}_\ell-\mathbf{k},\downarrow}^\dagger; c_{-\mathbf{q}_\ell+\mathbf{k},\downarrow}, -c_{\mathbf{q}_\ell-\mathbf{k},\uparrow}^\dagger)^T$ for each pair of nodes at opposite momenta:

$$\begin{aligned} \mathcal{H}_{\text{eff}} &= \sum_{\ell,\mathbf{k}} \Psi_{\ell\mathbf{k}}^\dagger H_{\ell\mathbf{k}} \Psi_{\ell\mathbf{k}}, \quad H_{\ell\mathbf{k}} = (\mathbf{n}_{\ell\mathbf{k}} \cdot \vec{\tau})\sigma_z, \quad (1) \\ \mathbf{n}_{\ell\mathbf{k}} &= (\text{Re}\Delta_{\mathbf{q}_\ell+\mathbf{k}}, -\text{Im}\Delta_{\mathbf{q}_\ell+\mathbf{k}}, \xi_{\mathbf{q}_\ell+\mathbf{k}}) \\ &= \sum_{\alpha=x,y} k_\alpha \vec{v}_\alpha^\ell + O(|\mathbf{k}|^2), \end{aligned}$$

where $\Delta_{\mathbf{k}}$ is the pairing gap function and $\xi_{\mathbf{k}}$ is the kinetic energy. $\vec{\tau}$ and $\vec{\sigma}$ are Pauli matrices operating in the particle-hole (Nambu) and spin sectors respectively. For simplicity, we set the velocity $v^\ell = 1$ hereafter. A particle-hole unitary rotation $U \equiv \exp[i\vec{\phi}_\ell \cdot \vec{\tau}]$ turns $H_{\ell\mathbf{k}}$ into $U^\dagger H_{\ell\mathbf{k}} U = (k_1\tau_x + k_2\tau_y)\sigma_z$ where $k_{1,2}$ are linearly-independent combinations of k_x and k_y [50].

Let's focus on a single ℓ -th pair of nodes at $\pm \mathbf{q}_\ell$. Clearly, a gap will be generated by adding a generic mass term $\tau_0(\sigma_x \text{Re}M - \sigma_y \text{Im}M)$, where M is a complex order

parameter, in the Hamiltonian for this pair of nodes,

$$U^\dagger H'_{\ell\mathbf{k}} U = (k_1 \tau_x + k_2 \tau_y) \sigma_z + \tau_0 (\sigma_x \text{Re} M - \sigma_y \text{Im} M). \quad (2)$$

This is nothing but the effective Hamiltonian for s -wave superconductivity on the surface of a 3D topological insulator with M playing the role of the superconducting order parameter [18]. It is known that the latter contains a single MBS in its vortex core. In the present context of singlet nodal superconductors, the physical origin of the local order M turns out to be a *non-collinear* (co-planar) magnetic order described by

$$\begin{aligned} \mathcal{H}_{cp} &= \sum_{\mathbf{r}} [M(S_{\mathbf{r}}^x + iS_{\mathbf{r}}^y)e^{i2\mathbf{q}_0 \cdot \mathbf{r}} + h.c.] \\ &= \sum_{\ell\mathbf{k}} M c_{\mathbf{q}_\ell + \mathbf{k} + \mathbf{q}_0, \uparrow}^\dagger c_{\mathbf{q}_\ell + \mathbf{k} - \mathbf{q}_0, \downarrow} + h.c., \end{aligned} \quad (3)$$

where $S_{\mathbf{r}}^a = \sum_{\alpha, \beta} c_{\mathbf{r}, \alpha}^\dagger \sigma_{\alpha, \beta}^a c_{\mathbf{r}, \alpha} / 2$, $a = x, y, z$ are the electron spin operators at lattice site \mathbf{r} . When the ordering wave vector $2\mathbf{q}_0$ connects the pair of nodes located at $\pm\mathbf{q}_\ell$, the magnetic scattering generates precisely the mass term in Eq. (2). Remarkably, this non-collinear magnetic order drives the nodal superconductor into a non-Abelian topological state since, among the two (even and odd) combinations $c_{\mathbf{k}, e(o)} \equiv \frac{1}{\sqrt{2}}(c_{\mathbf{q}_\ell + \mathbf{k}, \uparrow} \pm c_{-\mathbf{q}_\ell + \mathbf{k}, \downarrow})$, the odd-combination is driven into the weak-pairing phase [8] by the mass gap, while the even-combination enters a strong-pairing phase. The situation is analogous to a doubled-layer $\nu = 1/2$ fractional quantum Hall system, where an Abelian (331) state can be driven to a non-Abelian pfaffian state by a tunneling term between the layers [8, 30, 31]. In contrast to the pair of nodes with opposite momenta connected by the magnetic ordering vector $2\mathbf{q}_0$, the other nodal fermions are spin-flip scattered either to finite energy states away from the Fermi level or, in certain special cases, to different nodes not connected by the pairing part. As a result, they either remain gapless or be gapped out in the magnetic sector. We note that the existence of a single MBS will not be affected by the presence of other nodal excitations [23].

On general grounds, the non-collinear magnetic order can be realized in a frustrated system from the residual spin-spin interactions between the nodal fermions and coexists with superconductivity. We stress that it is crucial to require the magnetic order to be *non-collinear*: a collinear spin order such as

$$\begin{aligned} \mathcal{H}_{cl} &= 2m \sum_{\mathbf{r}} S_{\mathbf{r}}^x \cos(2\mathbf{q}_0 \cdot \mathbf{r}) \\ &= \sum_{\ell\mathbf{k}} \sum_{\sigma} m c_{\mathbf{q}_\ell + \mathbf{k} + \mathbf{q}_0, \sigma}^\dagger c_{\mathbf{q}_\ell + \mathbf{k} - \mathbf{q}_0, \sigma} + h.c., \end{aligned} \quad (4)$$

will not only drive the Nambu pair $(c_{\mathbf{q}_0 + \mathbf{k}, \uparrow}, c_{-\mathbf{q}_0 - \mathbf{k}, \downarrow}^\dagger)$, but also $(c_{-\mathbf{q}_0 + \mathbf{k}, \uparrow}, c_{\mathbf{q}_0 - \mathbf{k}, \downarrow}^\dagger)$ into the weak-pairing phase. This amounts to two copies of weak-pairing $p + ip$ superconductors. Thus, there will be two MBSs in the vortex

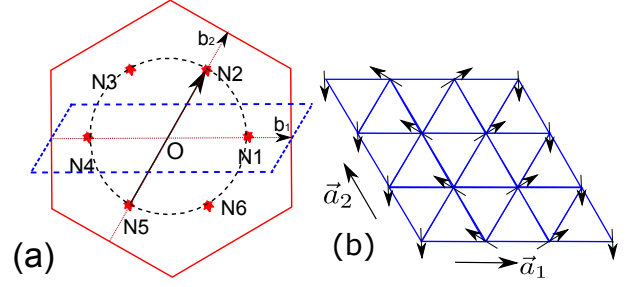


FIG. 1: (color online) (a) The 1st BZ of the triangular lattice and the 6 nodes (N_i) of the 2nd NN $d + id$ pairing gap function. The normal state hole FS (dashed circle) crosses the gap nodes at doping x_c for the nodal chiral superconductor. The arrow indicates the momentum of the 1×3 magnetic order with the magnetic zone shown by dashed parallelogram. (b) The spin configuration of the 1×3 non-collinear magnetic order. $\vec{a}_{1,2}$ are two primitive lattice vectors. The reciprocal vectors are $\vec{b}_{1,2}$ with the convention $\vec{a}_i \cdot \vec{b}_j = \delta_{i,j}$.

core and two counter-propagating Majorana modes on the edge. The two branches will scatter with each other and open up a gap in the edge spectrum. As a result, there will be no MBS in a nodal superconductor with collinear magnetic order.

In the presence of the non-collinear magnetic order (3), both inversion symmetry and spin rotational symmetry are broken and thus the spin-singlet pairing can mix with spin triplet pairing. When the triplet pairing amplitude is small compared with $|M|$, the system will stay in the gapped non-Abelian topological phase. In the opposite limit, a dominant one-component chiral triplet pairing state is well known to be in the non-abelian weak-pairing phase [8, 9]. Therefore we expect that the non-Abelian topological superconductor to be stable against the mixing between singlet and triplet pairing. In the following we shall demonstrate the above general discussions by two specific examples on the triangular and the square lattices.

We start with the nodal chiral superconductor with coplanar 1×3 magnetic order on the triangular lattice. Nodal chiral superconductors were proposed in the context of the sodium cobaltate superconductivity [24]. The sodium cobaltate (Na_xCoO_2) is a layered, strongly correlated triangular lattice electron system which becomes a superconductor upon water-intercalation at low temperatures [32]. Recent NMR measurements find strong evidence for singlet pairing [25, 33, 34] with nodal excitations at a critical doping $x_c \approx 0.26$ [34], which can be explained by the nodal $d + id$ pairing state [24]. Specifically, 2nd nearest neighbor (NN) $d + id$ pairing was argued to be the dominant pairing channel on the electron doped triangular lattice where the complex gap function has 6 isolated zeros inside the 1st Brillouin zone (BZ). The Fermi surface (FS) crosses these nodes at a critical doping concentration x_c producing 6 Dirac points as shown

in Fig. 1(a). The superconducting states at $x < x_c$ and $x > x_c$ are separable by a topological phase transition. We therefore consider a simple effective pairing model described by the Hamiltonian,

$$\mathcal{H} = \sum_{\mathbf{k}\sigma} \xi_{\mathbf{k}} c_{\mathbf{k}\sigma}^\dagger c_{\mathbf{k}\sigma} + \sum_{\mathbf{k}} (\Delta_{\mathbf{k}} c_{\mathbf{k}\uparrow} c_{-\mathbf{k}\downarrow} - h.c.), \quad (5)$$

where $\xi_{\mathbf{k}}$ is the dispersion for electrons hopping with amplitudes $(t_1, t_2, t_3) = (-202, 35, 29)$ meV between the first 3 nearest-neighbors (NNs) [24]. $\Delta_{\mathbf{k}} = 2\Delta_2 [\cos(k_1 - k_2) + e^{i2\pi/3} \cos(2k_1 + k_2) + e^{i4\pi/3} \cos(k_1 + 2k_2)]$ is the 2nd NN $d + id$ pairing gap function in the basis $\mathbf{k} = k_1 \vec{b}_1 + k_2 \vec{b}_2$ shown in Fig. 1(a) where the 6 Dirac nodes (N_i , $i = 1, \dots, 6$) are located at $(k_1, k_2) = \pm(2\pi/3, 0)$, $\pm(0, 2\pi/3)$, and $\pm(2\pi/3, -2\pi/3)$. Such a $d + id$ superconductor exhibits quantized spin Hall conductance [8] associated with the winding number W of the unit vector $\hat{n}_{\mathbf{k}} = (\text{Re}\Delta_{\mathbf{k}}^{(2)}, -\text{Im}\Delta_{\mathbf{k}}^{(2)}, \xi_{\mathbf{k}})/E_{\mathbf{k}}$ where $E_{\mathbf{k}} = \sqrt{\xi_{\mathbf{k}}^2 + |\Delta_{\mathbf{k}}^{(2)}|^2}$. When the FS lies inside the Dirac points ($x > x_c$), $W = -2$ and there are two counter-clockwise-propagating chiral fermions on the edge; each is charge neutral but carries spin $\hbar/2$ [24]. When the FS encloses the six gap nodes ($x < x_c$), $W = 4$ and there are four spin-carrying chiral fermions on the edge.

Remarkably, a non-collinear magnetic order described by \mathcal{H}_{cp} in Eq. (3), with the vector $2\mathbf{q}_0$ pointing from N_{i+3} to N_i (Fig. 1a), produces a mass gap for the nodal fermions as discussed above. The magnetic order corresponds to the 1×3 coplanar pattern shown in Fig. 1(b). The nodal chiral superconductor is thus turned into a non-Abelian topological superconductor with a winding number $W = +1$, which is formally identical to a $p + ip$ superconductor [8] and supports a single MBS in the vortex core and on the sample edge. To demonstrate the latter, we calculate explicitly the edge spectrum of such a non-collinear magnetic superconductor described by $\mathcal{H} + \mathcal{H}_{cp}$ with two parallel edges along the (1,1) direction. The results are shown in Fig. 2 for $\Delta_2 = 150$ meV and magnetic mass $M = 100$ meV. The bulk excitations are completely gapped, due to the fact that the magnetic scattering wave vector $2\mathbf{q}_0$ not only connects the Nambu pair (N_5, N_2) but also (N_3, N_4) and (N_1, N_6) in the magnetic sector. The in-gap edge states are separated from the bulk continuum. The central result is that there is a single branch of gapless edge mode of a single MBS crossing $k = 0$ localized at the two edges respectively. We verified that, as discussed in the generic case above, a collinear magnetic order described by \mathcal{H}_{cl} in Eq. (4) will not create a MBS in the edge spectrum, although the bulk excitations are fully gapped (see supplemental materials).

A natural question rises: how does the 1×3 non-collinear magnetic order arise microscopically on the triangular lattice? To this end, we consider the 2nd NN antiferromagnetic Heisenberg model, *i.e.* the J_2 model,

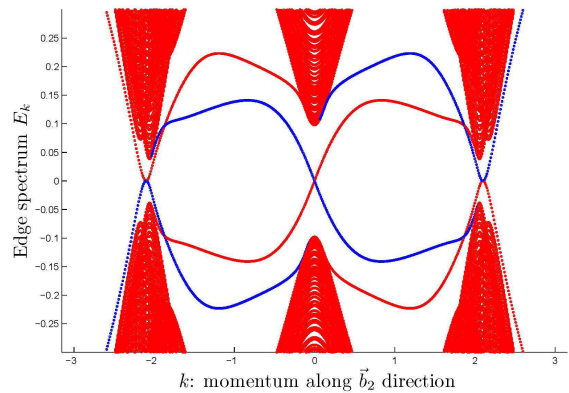


FIG. 2: (color online) Edge state spectra as a function of momentum k along \vec{b}_2 direction in the magnetic zone as shown in Fig. 1. The in-gap edge states are separated from the bulk continuum. Blue and red lines correspond to the edge states localized on the two separate edges respectively. Note that there is a single counter-clockwise-propagating zero-energy MBS at $k = 0$.

on the triangular lattice. The classical ground states of the J_2 model is well-known to have 3×3 non-collinear magnetic order [35, 36]: on each of the three sublattices connected by 2nd-NN bonds the spins exhibit 120 degree coplanar order. There is a large ground state degeneracy at the classical level from the relative spin orientations on the three sublattices. Such a 3×3 noncollinear magnetic order as a classical ground state of J_2 model already induces a single MBS crossing $k = 0$ in the edge spectrum, as shown in the supplementary materials. Quantum fluctuations would further lift this degeneracy at classical level through the order-due-to-disorder mechanism [37–39], such that the true quantum ground state has 1×3 order. We have carried out a Schwinger-boson large- S expansion study (see supplementary materials) of the spin- S Heisenberg J_2 model and found that when S is larger than a critical value $S_c \approx 0.17$ (such as for spin-1/2), the system develops the 1×3 non-collinear order as shown in Fig. 1(b). This suggests that if the residual interaction between the nodal fermions is dominated by the 2nd NN Heisenberg exchange J_2 , then the 1×3 non-collinear magnetic order is likely to develop with the wave vector $2\mathbf{q}_0$ connecting the gap nodes with opposite momenta as shown in Fig. 1. Even more intriguingly, to the extent that J_2 would favor a 2nd NN $d + id$ resonance valence bond pairing state, it is likely that both the nodal chiral superconductor and the non-collinear magnetic order can emerge from the same exchange interaction in a doped t - J_2 model.

We turn to the 2nd example of a more familiar nodal $d_{x^2-y^2}$ superconductor with (Q_0, Q_0) coplanar magnetic order on the square lattice. The Hamiltonian has the same form as \mathcal{H} in Eq. (5), but with the dispersion $\xi_{\mathbf{k}} = -2t [\cos(k_1 + k_2) + \cos(k_1 - k_2)] - \mu$ for NN hop-

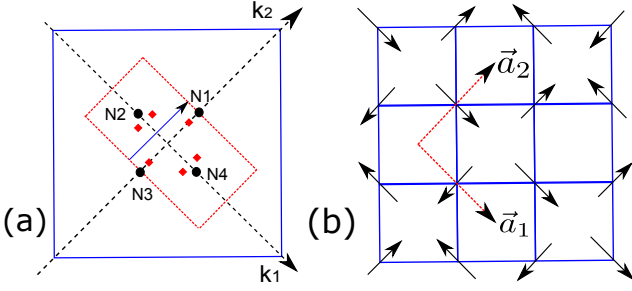


FIG. 3: (color online) (a) The 1st BZ of the square lattice. Black circles denote the four nodal points (N_i) where the FS intersects the nodal lines of the NN $d_{x^2-y^2}$ pairing gap function. The non-collinear magnetic order with momentum $(\pi/2, \pi/2)$ (shown by the arrow) turns the node-structure into the 6 red diamonds inside the magnetic zone (red rectangle). (b) The spin configuration of the $(\pi/2, \pi/2)$ non-collinear magnetic order. $\vec{a}_{1,2}$ represent two primitive vectors. The reciprocal vectors are $\vec{b}_{1,2}$ with $\vec{a}_i \cdot \vec{b}_j = \delta_{i,j}$. Along \vec{a}_2 direction the unit cell is doubled due to magnetic order.

ping t , and the NN $d_{x^2-y^2}$ pairing gap function $\Delta_{\mathbf{k}} = 2\Delta_1 [\cos(k_1 + k_2) - \cos(k_1 - k_2)]$. The momentum is defined as $\mathbf{k} = k_1\vec{b}_1 + k_2\vec{b}_2$ as shown in Fig. 3, where four nodal points arise from the crossing of the FS with the nodal lines of the gap function: $N_{1,3} : (k_1 = 0, k_2 = \pm q_0)$ and $N_{2,4} : (k_1 = \pm q_0, k_2 = 0)$ with $q_0 = \arccos(-\frac{\mu}{4t})$. A non-collinear magnetic order described by \mathcal{H}_{cp} in Eq. (3) with ordering momentum $\mathbf{Q}_0 = 2\mathbf{q}_0 = 2q_0\vec{b}_2$ gaps out the $(c_{N_3,\uparrow}, c_{N_1,\downarrow}^\dagger)$ branch and creates a single MBS. Fig. 3 shows a specific example with $\mu = -2\sqrt{2}t$ and $q_0 = \pi/4$, together with the spin configurations. In this case, the commensurate magnetic order cannot gap out all nodal excitations since the Hamiltonian is still invariant under time reversal followed by a lattice translation [40]. As shown in Fig. 3(a), the non-collinear magnetic order splits the original four spin-degenerate nodal points (black circles) into 6 non-degenerate nodes (red diamonds). The vanished pair of nodes is gapped out by the magnetic mass (3) and enters the weak-pairing phase. The calculated edge spectra along the (1,1) direction is shown in Fig. 4 near the magnetic zone boundary. It confirms the existence of zero energy MBS localized on the parallel edges. Similar results are obtained at other commensurate values of q_0 such as $q_0 = \pi/3$. Since the gapless bulk excitations are located at different momenta, the MBS near $k_2 = \pi$ is expected to be stable against impurities and the mixing with bulk excitations [23]. For a generic doping, q_0 is incommensurate with the lattice and a corresponding incommensurate non-collinear magnetic order would open up a full gap for the bulk excitations and leave the edge states as the only low-energy modes.

A surprising and remarkable feature seen in Fig. 4 is that the Majorana mode on the edge is dispersionless, i.e. it is localized and does not possess a chirality. It turns out that the chirality of the Majorana mode on the

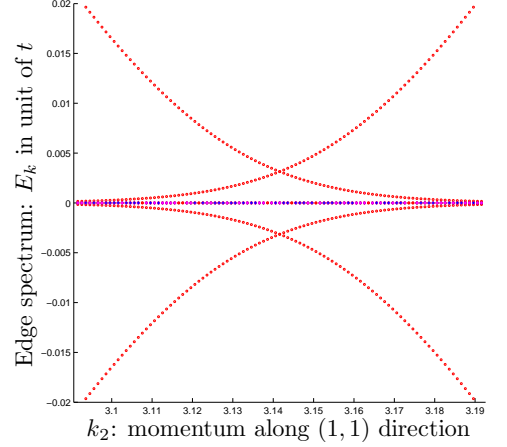


FIG. 4: (color online) Edge spectra as a function of momentum k_2 along the (1,1) direction of the magnetic zone for a NN $d_{x^2-y^2}$ superconductor with $(\pi/2, \pi/2)$ non-collinear magnetic order. The spectrum is zoomed in around $k_2 = \pi$ where a flat band of zero energy states are localized on the two edges (blue and magenta), corresponding to the MBS. Red dispersing lines are the bulk states and the two nodal points in the bulk excitations are located at $k_2 \approx \pi \pm 0.04$.

edge crucially depends on the symmetry of the pairing order parameter $\Delta_{\mathbf{k}}$ in (1). The chirality of the edge mode associated with the ℓ -th pair of gap nodes can be defined as $C^\ell = \text{sign}[\hat{z} \cdot (\vec{v}_x^\ell \times \vec{v}_y^\ell)]$, where $\vec{v}_{x,y}^\ell$ are the velocities defined in (1). It is straightforward to verify that this definition is invariant under a global $U(1)$ rotation $c_{\mathbf{k},\sigma} \rightarrow e^{i\theta} c_{\mathbf{k},\sigma}$. For a singlet nodal superconductor that preserves the time-reversal symmetry, which is the case for the $d_{x^2-y^2}$ superconductor, the chirality of the edge mode $C = 0$ and hence the non-dispersing Majorana edge mode in FIG. 4. However in the presence of the magnetic order (3), a time reversal symmetry breaking pairing term can be induced. We verified that adding a small imaginary part in Δ_1 indeed generates a single MBS on the edge that disperses across $k_2 = \pi$ with certain chirality (see supplementary material).

It is possible to realize this non-collinear magnetic order in the microscopic Heisenberg J_1 - J_2 - J_3 model on the square lattice. The classical ground state of the J_1 - J_2 - J_3 model is a non-collinear one with momenta $\mathbf{Q}_0 = Q_0\vec{b}_{1,2}$ where $\cos(Q_0) = -J_1/(2J_2 + 4J_3)$ for $4J_3 + 2J_2 \geq J_1$ and $J_3 \geq J_2/2$ [41, 42]. There are numerical evidence that the latter survives in the quantum $S = 1/2$ Heisenberg J_1 - J_2 - J_3 model in a wide parameter range [43, 44]. Therefore we expect that the non-Abelian phase of a nodal d -wave superconductor coexisting with $\mathbf{Q}_0 = Q_0\vec{b}_{1,2}$ non-collinear magnetic order may be realized in certain parameter regime of the doped t - J_1 - J_2 - J_3 model.

In summary, we proposed a new type of non-Abelian topological superconductors. They emerge when spin-singlet superconductors with isolated nodes coexist with

non-collinear magnetic order with the ordering vector connecting the nodes at opposite momenta due to the exchange interaction between the nodal fermions. Majorana fermions arise in the vortex core and on the edge of such magnetic superconductors. Since magnetism and unconventional superconductivity are common features of strong correlation, our findings suggest searching for the non-Abelian MBSs in correlated electronic materials with magnetic frustration and nodal superconductivity.

We thank Sen Zhou for useful discussions. This work is supported in part by NSF DMR-0704545 and DOE DE-FG02-99ER45747.

Supplementary Materials

A. Noncollinear magnetic order of J_2 Heisenberg model on triangular lattice

Due to geometric frustration, the triangular lattice antiferromagnet has long been considered as a promising candidate for realizing the spin liquid state [45]. These spin disordered states are different from conventional symmetry-breaking phases and its low-energy excitations are deconfined fractionalized quasiparticles (such as bosonic/fermionic spinons which carry spin but not electric charge). Strong quantum fluctuations at low temperatures may stabilize such disordered states; whereas in the large- S classical limit, various symmetry breaking magnetic ordered states develop with their low-energy physics dominated by Goldstone modes associated with the broken symmetry, *i.e.* spin waves or magnons. A well-known example is the zero-flux state introduced by Sachdev [46] in the Schwinger-boson representation. As the spin S (or the occupation number of bosonic spinon per site) increases to a critical value [47], the spinons at the zone corner condense, leading to the 120 degree ordered state as predicted for the classical Heisenberg J_1 model on the triangular lattice. In general a continuous quantum phase transition between a disordered spin liquid and a non-collinear magnetically ordered phase can be described by Bose condensation of spinons [48].

Our strategy here is to use the Schwinger-boson representation to study the Z_2 spin liquids for the 2nd nearest neighbor (NN) J_2 Heisenberg model on the triangular lattice. We then track down the pattern of the non-collinear magnetic order by studying the Bose condensation of spinons in the neighborhood of the spin liquid state using the Schwinger boson mean field theory.

Schwinger-boson representation of Z_2 spin liquids in triangular lattice J_2 model

In the Schwinger-boson representation the spin operators \mathbf{S}_r on lattice site r are written in terms of Schwinger

bosons $b_{r\alpha}$

$$\mathbf{S}_r = \frac{1}{2} \sum_{\alpha,\beta=\uparrow,\downarrow} b_{r,\alpha}^\dagger \vec{\sigma}_{\alpha,\beta} b_{r,\beta} \quad (6)$$

where $\vec{\sigma}$ denotes the three Pauli matrices. The spin value S is fixed by the constraint

$$\sum_{\alpha=\uparrow,\downarrow} b_{r,\alpha}^\dagger b_{r,\alpha} = \kappa = 2S, \quad \forall r. \quad (7)$$

Here $\kappa = 2S$ is a parameter measuring the strength of quantum fluctuations in the system and $\kappa \rightarrow +\infty$ corresponds to the classical limit. Consider two sites i and j , there are only two bond variables that preserve the spin rotational symmetry

$$\begin{aligned} \hat{B}_{ij} &= \frac{1}{2} \sum_{\alpha} b_{i,\alpha}^\dagger b_{j,\alpha} \\ \hat{A}_{ij} &= \frac{1}{2} \sum_{\alpha\beta} \epsilon_{\alpha\beta} b_{i,\alpha}^\dagger b_{j,\beta}, \end{aligned}$$

where $\epsilon_{\alpha\beta}$ is the rank-2 fully anti-symmetric tensor. Thus, a generic Heisenberg Hamiltonian can be written as

$$H = \sum_{i,j} J_{ij} \mathbf{S}_i \cdot \mathbf{S}_j = \sum_{i,j} J_{ij} (-\hat{A}_{ij}^\dagger \hat{A}_{ij} + \hat{B}_{ij}^\dagger \hat{B}_{ij}). \quad (8)$$

At the mean-field level, the pairing amplitudes $A_{ij} \equiv \langle \hat{A}_{ij} \rangle = -A_{ji}$ and the hopping amplitudes $B_{ij} \equiv \langle \hat{B}_{ij} \rangle = B_{ji}$ where A_{ij}, B_{ij} are complex variational parameters. Enforcing the constraint (7) globally by a chemical potential μ , we obtain the mean-field Hamiltonian

$$\begin{aligned} H_{MF} &= \sum_{i,j} J_{ij} (-A_{ij} \hat{A}_{ij} + B_{ij} \hat{B}_{ij} + h.c.) \\ &+ \sum_{i,j} J_{ij} (|A_{ij}|^2 - |B_{ij}|^2) - \mu \sum_r (b_{r,\alpha}^\dagger b_{r,\alpha} - \kappa) \end{aligned} \quad (9)$$

Different types of the spatial “patterns” of the amplitudes $\{A_{ij}, B_{ij}\}$ correspond to different universality classes of the Z_2 spin liquids. They are characterized by different symmetry-protected topological orders and classified by the projective symmetry group (PSG) [49]. In Ref. 47, all different Z_2 spin liquids preserving the lattice symmetry on the triangular lattice are classified in the Schwinger-boson representation. There are in total 8 different PSGs on an isotropic triangular lattice, corresponding to 8 different universality classes of the Z_2 spin liquids.

Let's focus on those spin liquid states that are possible ground states in the 2nd NN J_2 Heisenberg model on an isotropic triangular lattice. We require the 2nd NN mean-field pairing amplitudes to be nonzero: $A_{ij} \neq 0$ for $\langle \langle ij \rangle \rangle$. This constraint excludes 6 of the 8 possible Z_2 PSGs. Therefore we have only two different Z_2 spin liquids with nonzero 2nd NN A_{ij} 's: they are labeled as the π -flux state (following the name given in Ref. 47) and 0-flux-2 state (in order to distinguish from the zero-flux state in Ref. 47). The 0-flux-2 state corresponds to the

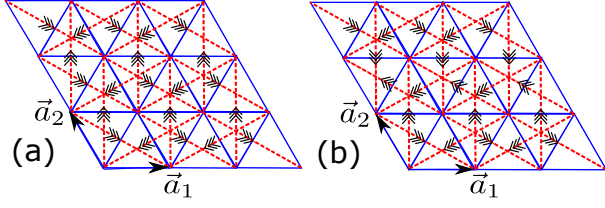


FIG. 5: (color online) The sign structure of 2nd NN pairing amplitudes $A_{ij} = \frac{1}{2}(b_{i\uparrow}b_{j\downarrow} - b_{i\downarrow}b_{j\uparrow})$ for the two different Z_2 spin liquids: (a) 0-flux-2 state and (b) π -flux state. Specifically, writing $A_{ij} = \pm iA_2$ with A_2 a constant, then the plus sign is assigned if $i \rightarrow j$ is along the direction of the triple arrows. $\vec{a}_{1,2}$ are two primitive lattice vectors. Note that the π -flux state breaks translation symmetry along the \vec{a}_2 direction and doubles the unit cell.

Z_2 PSG solution $p_1 = 0$, $p_2 = p_3 = 1$ in the notation of Ref. 47. Among them the π -flux state doesn't allow 2nd NN hopping terms, *i.e.* $B_{ij} = 0$ for all $\langle\langle ij \rangle\rangle$. The 0-flux-2 state, however, does allow uniform real 2nd NN hopping, *i.e.* $B_{ij} \equiv B_2 \in \mathbb{R}$ for all $\langle\langle ij \rangle\rangle$. For both phases, the 2nd NN pairing amplitudes can be made purely imaginary by a gauge choice, with their spatial sign structures shown in Fig. 5.

We carry out self-consistent calculations of the mean-field Hamiltonian (9) for both the π -flux and the 0-flux-2 states. For simplicity we only include the 2nd NN pairing amplitudes for the 0-flux-2 state. Thus, strictly speaking the obtained ground state energy for the 0-flux-2 state gives an upper bound of the actual energy. The comparison of the ground state energy (or zero-temperature free energy) for the two states are shown in Fig. 6, which shows that the 0-flux-2 state has a lower energy than the π -flux state. A nonzero 2nd NN hopping amplitudes B_2 would lower the energy of the 0-flux-2 state even further. Thus the lowest energy Z_2 spin liquid state in the triangular lattice J_2 model should be the 0-flux-2 state which, as we will show below, is stable against spin order when the quantum parameter is smaller than $\kappa_c \approx 0.34$ (see Fig. 6).

Spinon condensation and the magnetic order in triangular lattice J_2 Heisenberg model

Now we show how to extract the magnetic ordering pattern in the 0-flux-2 state when κ becomes large. We choose $\vec{b}_{1,2}$ to be the reciprocal lattice vector which satisfies $\vec{a}_i \cdot \vec{b}_j = \delta_{i,j}$, $i, j = 1, 2$ where $\vec{a}_{1,2}$ are the primitive vectors shown in Fig. 5. Expressing the momentum as $\mathbf{k} = k_1\vec{b}_1 + k_2\vec{b}_2$, the mean-field Hamiltonian can be writ-

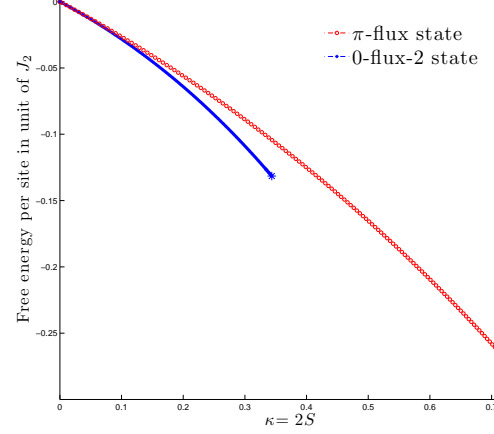


FIG. 6: (color online) The mean-field ground state energy per site $E_{gs}/(N_s J_2) = -3|A_2|^2$ of the two Z_2 spin liquid states in the J_2 Heisenberg model on the triangular lattice. Blue asterisks denote 0-flux-2 state and red circles denote π -flux state. Apparently 0-flux-2 state has lower energy than its competitor π -flux state and should be the ground state of J_2 model for $\kappa \leq 0.34$. When the quantum parameter $\kappa = 2S$ increases and becomes larger than critical values $\kappa_c(0\text{-flux-2}) \approx 0.34$ and $\kappa_c(\pi\text{-flux}) \approx 0.75$, the spin system goes through a phase transition from spin liquid phases to magnetic ordered phases.

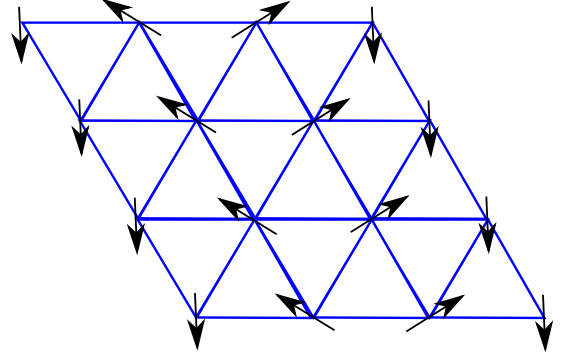


FIG. 7: (color online) The spin configuration of the 1×3 coplanar magnetic order in a $S = 1/2$ Heisenberg J_2 model on the triangular lattice, obtained from spinon condensation in the 0-flux-2 state.

ten as

$$H_{MF} = \sum_{\mathbf{k}} \begin{bmatrix} b_{\mathbf{k},\uparrow}^\dagger \\ b_{-\mathbf{k},\downarrow} \end{bmatrix}^T \begin{pmatrix} -\mu & J_2 A_2 g_{\mathbf{k}}^{(2)} \\ J_2 A_2 g_{\mathbf{k}}^{(2)} & -\mu \end{pmatrix} \begin{bmatrix} b_{\mathbf{k},\uparrow} \\ b_{-\mathbf{k},\downarrow}^\dagger \end{bmatrix} + N_s \left[\mu(\kappa + 1) + 3J_2 |A_2|^2 \right], \quad (10)$$

where N_s is the number of lattice sites and

$$g_{\mathbf{k}}^{(2)} = -\sin(k_1 - k_2) - \sin(k_1 + 2k_2) + \sin(2k_1 + k_2)$$

is the 2nd NN pairing structure factor corresponding to Fig. 5(a). The spinon dispersion, obtained from Eq. (10),

$$\lambda_{\mathbf{k}} = \sqrt{\mu^2 - |J_2 A_2 g_{\mathbf{k}}^{(2)}|^2} \quad (11)$$

has 6 minima at $(k_1, k_2) = \pm(2\pi/3, 0)$, $\pm(0, 2\pi/3)$ and $\pm(2\pi/3, -2\pi/3)$ which coincide with the 6 gap nodes $\{N_i\}$ of the 2nd NN $d + id$ pairing gap function [51]. We denote the momenta at points N_i as \mathbf{k}_i . As the quantum parameter κ increases, the chemical potential μ decreases and the minima of the spinon bands $\min\{\lambda_{\mathbf{k}}\} = \sqrt{\mu^2 - 27|J_2 A_2|^2/4}$ approach zero from the positive side. When $\mu = 3\sqrt{3}J_2 A_2/2$ the band minima touch zero, the spinons at the 6 momentum points condense into

$$\begin{bmatrix} \langle b_{\mathbf{k}_i, \uparrow} \rangle \\ \langle b_{-\mathbf{k}_i, \downarrow} \rangle \end{bmatrix} = c_i \begin{bmatrix} 1 \\ (-1)^i \end{bmatrix}, \quad i = 1, 2, 3, 4, 5, 6, \quad (12)$$

where c_i are complex numbers. The spatial configuration of the spinons is then given by

$$\begin{aligned} \Psi_{\mathbf{r}} &\equiv \begin{bmatrix} \langle b_{\mathbf{r}, \uparrow} \rangle \\ \langle b_{\mathbf{r}, \downarrow} \rangle \end{bmatrix} = \sum_{i=1}^6 e^{i\mathbf{k}_i \cdot \mathbf{r}} \begin{bmatrix} \langle b_{\mathbf{k}_i, \uparrow} \rangle \\ \langle b_{\mathbf{k}_i, \downarrow} \rangle \end{bmatrix} \\ &= \phi_1 U_1 \begin{bmatrix} \omega^x \\ \omega^{-x} \end{bmatrix} + \phi_2 U_2 \begin{bmatrix} \omega^y \\ \omega^{-y} \end{bmatrix} + \phi_3 U_3 \begin{bmatrix} \omega^{y-x} \\ \omega^{x-y} \end{bmatrix} \end{aligned} \quad (13)$$

where $\mathbf{r} = x\vec{a}_1 + y\vec{a}_2$ is the position vector of a site and $\omega = \exp(i2\pi/3)$. In the above equation, $\phi_{1,2,3}$ are three positive constants and $U_{1,2,3}$ are three $SU(2)$ matrices with

$$\phi_i U_i = \begin{pmatrix} c_i & c_{i+3} \\ -c_{i+3}^* & c_i^* \end{pmatrix}, \quad i = 1, 2, 3.$$

The condensed spinons give rise to magnetic order and the corresponding spin configuration is

$$\begin{aligned} \mathbf{S}_{\mathbf{r}} &= \frac{1}{2} \Psi_{\mathbf{r}}^\dagger \vec{\sigma} \Psi_{\mathbf{r}} = \frac{1}{2} \text{Tr}[\Psi_{\mathbf{r}} \Psi_{\mathbf{r}}^\dagger \vec{\sigma}] \\ &= \frac{\phi_1^2}{2} \text{Tr} \left\{ \begin{bmatrix} 1 & \omega^{2x} \\ \omega^{-2x} & 1 \end{bmatrix} U_1^\dagger \vec{\sigma} U_1 \right\} \\ &+ \frac{\phi_2^2}{2} \text{Tr} \left\{ \begin{bmatrix} 1 & \omega^{2y} \\ \omega^{-2y} & 1 \end{bmatrix} U_2^\dagger \vec{\sigma} U_2 \right\} \\ &+ \frac{\phi_3^2}{2} \text{Tr} \left\{ \begin{bmatrix} 1 & \omega^{2(y-x)} \\ \omega^{2(x-y)} & 1 \end{bmatrix} U_3^\dagger \vec{\sigma} U_3 \right\}. \end{aligned} \quad (14)$$

In general, when all three ϕ_i 's are nonzero, the magnetic order has the 3×3 spatial pattern on the triangular lattice. More precisely, there are three sublattices connected by the 2nd-NN J_2 bonds: on every sublattice the spins form coplanar 120 degree order as in the NN J_1 Heisenberg model. When only one ϕ_i is nonzero, the corresponding spin configuration is the stripe-like 1×3 coplanar ordered shown in Fig. 7.

The classical ground state of the J_1 - J_2 Heisenberg model with $\alpha = J_2/J_1 > 1$ is known [35, 36] to have non-collinear magnetic order on the triangular lattice with

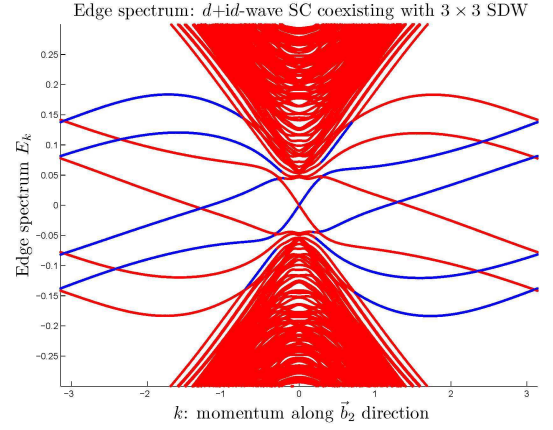


FIG. 8: (color online) Edge spectrum of 2nd-NN $d + id$ superconductor coexisting with an arbitrary 3×3 non-collinear magnetic order (14). Notations are the same as in Fig. 2 of the main text. Among the in-gap edge states separated from the bulk continuum, blue lines represent edge states on one edge, while red lines represent edge states on the other edge. The edge is along (1,1) direction. There is one single clockwise-propagating MBS crossing $k = 0$ in the magnetic zone. The data are obtained for $\Delta_2 = 150 \text{ meV}$ and magnetic mass $M = 100 \text{ meV}$ for all three ordering vectors.

the following momenta

$$\begin{aligned} \mathbf{k} &= (k_1, k_2) = \pm(Q_0, 0), \quad \pm(0, Q_0) \text{ and } \pm(Q_0, -Q_0), \\ Q_0 &= \arccos(-\frac{1}{2} - \frac{1}{2\alpha}). \end{aligned} \quad (15)$$

In the limit $\alpha \rightarrow +\infty$, they exactly correspond to the magnetic order (14) obtained by condensing spinons in the 0-flux-2 spin liquid state. These classical solutions have a large ground state degeneracy, due to the relative spin orientations between different 2nd-NN sublattices as mentioned earlier. When quantum fluctuations are considered, the degeneracy at the classical level will be lifted through the “order due to disorder” mechanism [37, 38]. Therefore the ground state of the quantum Heisenberg J_2 model is expected [39] to exhibit magnetic order with one ordering wavevector among those in (15). In other words, only one of the $\{c_i, i = 1, \dots, 6\}$ in (13) is nonzero and the corresponding spin configuration (14) is the 1×3 noncollinear order shown in Fig. 7.

B. Majorana fermions with 3×3 noncollinear magnetic order

It turns out that even for an arbitrary classical ground state (14) with a 3×3 non-collinear magnetic order, when it coexists with the 2nd NN $d + id$ superconductivity on the triangular lattice, there will still be a single Majorana bound state on the edge of the sample. An explicit example of the edge spectrum is shown in Fig. 8, where

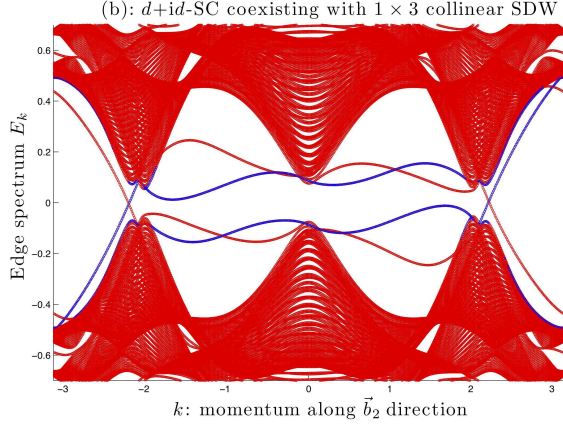


FIG. 9: (color online) The edge spectra with momentum k along \vec{b}_2 direction of a 2nd-NN $d + id$ superconductor coexisting with 1×3 *collinear* magnetic order with magnetization along \hat{z} direction. Notations are the same as in Fig. 2 of the main text. Note the absence of Majorana bound state in the spectrum. The data are obtained for pairing energy $\Delta_2 = 150$ meV and magnetic mass $m = 100$ meV for the collinear order.

a single Majorana mode is localized on each of the two parallel edges and disperses across $k = 0$.

C. Absence of Majorana fermions with collinear magnetic order

As discussed in the main text for the generic case, a collinear magnetic order described by \mathcal{H}_{cl} in Eq. (3) in the main text will not create a Majorana bound state in the vortex core or on the sample edge, although the bulk excitations are fully gapped. In Fig. 9, we show explicitly the absence of Majorana mode in the edge spectrum obtained for a 2nd-NN $d + id$ superconductor coexisting with 1×3 *collinear* magnetic order with magnetization along \hat{z} direction.

D. Chirality of Majorana edge mode

As discussed in the main text, when the pairing order parameter preserves time reversal symmetry the chiral of Majorana edge mode is $C = \text{sign}[\hat{z} \cdot (\vec{v}_x^\ell \times \vec{v}_y^\ell)] = 0$, corresponding to a dispersionless MBS on the edge, as shown in FIG. 4 for the NN real $d_{x^2-y^2}$ pairing on square lattice. However in the presence of a magnetic order, time reversal symmetry is broken and a small imaginary pairing term Δ_1 can be induced. This would result in a dispersing Majorana edge mode with $C = \pm 1$. Here we demonstrate this fact by calculating the edge spectrum of a $d_{x^2-y^2}$ pairing coexisting with $(\pi/2, \pi/2)$ non-collinear magnetic order, when a very small 2nd NN imaginary pairing term $\Delta_{\mathbf{k},1} = 0.02i \cos(k_1)$ is induced.

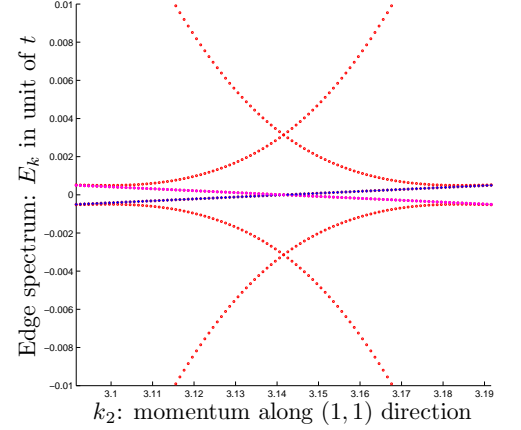


FIG. 10: (color online) Edge spectra as a function of momentum k_2 along the $(1,1)$ direction of the magnetic zone for a NN $d_{x^2-y^2}$ superconductor with $(\pi/2, \pi/2)$ non-collinear magnetic order. The spectrum is zoomed in around $k_2 = \pi$ where a flat band of zero energy states are localized on the two edges (blue and magenta), corresponding to the MBS. Red lines are the bulk states. Here we add a small 2nd NN imaginary pairing term $\Delta_{\mathbf{k},1} = 0.02i \cos(k_1)$.

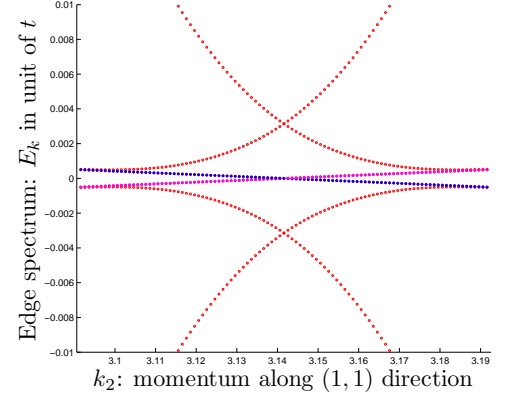


FIG. 11: (color online) Edge spectra as a function of momentum k_2 along the $(1,1)$ direction of the magnetic zone for a NN $d_{x^2-y^2}$ superconductor with $(\pi/2, \pi/2)$ non-collinear magnetic order. The spectrum is zoomed in around $k_2 = \pi$ where a flat band of zero energy states are localized on the two edges (blue and magenta), corresponding to the MBS. Red lines are the bulk states. Here we add a small 2nd NN imaginary pairing term $\Delta_{\mathbf{k},1} = -0.02i \cos(k_1)$.

pairing $\Delta_{\mathbf{k},1} = \pm 0.02i \cos(k_1)$ is induced. As shown in FIG. 10 and 11, the dispersionless MBS in FIG. 4 begins to disperse in the presence of the imaginary pairing term. When the sign of this imaginary pairing changes, the chirality of the Majorana edge mode changes accordingly.

* Present address: Department of Physics, University of California, Berkeley, CA 94720.

- [1] F. Wilczek, Nat Phys **5**, 614 (2009).
- [2] C. Nayak, S. H. Simon, A. Stern, M. Freedman, and S. Das Sarma, Rev. Mod. Phys. **80**, 1083 (2008).
- [3] M. Z. Hasan and C. L. Kane, Rev. Mod. Phys. **82**, 3045 (2010).
- [4] X.-L. Qi and S. C. Zhang, arXiv:1008.2026v1 (2010).
- [5] G. Moore and N. Read, Nuclear Physics B **360**, 362 (1991).
- [6] C. Nayak and F. Wilczek, Nuclear Physics B pp. 529–553 (1996).
- [7] E. Fradkin, C. Nayak, A. Tsvelik, and F. Wilczek, Nuclear Physics B **516**, 704 (1998).
- [8] N. Read and D. Green, Phys. Rev. B **61**, 10267 (2000).
- [9] D. A. Ivanov, Phys. Rev. Lett. **86**, 268 (2001).
- [10] M. Stone and S.-B. Chung, Phys. Rev. B **73**, 014505 (2006).
- [11] X. G. Wen and Q. Niu, Phys. Rev. B **41**, 9377 (1990).
- [12] X. G. Wen, Phys. Rev. Lett. **66**, 802 (1991).
- [13] A. Y. Kitaev, Annals of Physics **303**, 2 (2003).
- [14] S. Das Sarma, M. Freedman, and C. Nayak, Phys. Rev. Lett. **94**, 166802 (2005).
- [15] Y.-M. Lu, Y. Yu, and Z. Wang, Phys. Rev. Lett. **105**, 216801 (2010).
- [16] V. Gurarie, L. Radzihovsky, and A. V. Andreev, Phys. Rev. Lett. **94**, 230403 (2005).
- [17] N. R. Cooper and G. V. Shlyapnikov, Phys. Rev. Lett. **103**, 155302 (2009).
- [18] L. Fu and C. L. Kane, Phys. Rev. Lett. **100**, 096407 (2008).
- [19] T. D. Stanescu, J. D. Sau, R. M. Lutchyn, and S. Das Sarma, Phys. Rev. B **81**, 241310 (2010).
- [20] M. Sato, Y. Takahashi, and S. Fujimoto, Phys. Rev. Lett. **103**, 020401 (2009).
- [21] J. D. Sau, R. M. Lutchyn, S. Tewari, and S. Das Sarma, Phys. Rev. Lett. **104**, 040502 (2010).
- [22] J. Alicea, Phys. Rev. B **81**, 125318 (2010).
- [23] M. Sato and S. Fujimoto, Phys. Rev. Lett. **105**, 217001 (2010).
- [24] S. Zhou and Z. Wang, Phys. Rev. Lett. **100**, 217002 (2008).
- [25] G.-q. Zheng, K. Matano, R. L. Meng, J. Cmaidalka, and C. W. Chu, Journal of Physics: Condensed Matter **18**, L63 (2006).
- [26] C. C. Tsuei and J. R. Kirtley, Rev. Mod. Phys. **72**, 969 (2000).
- [27] C. Pfleiderer, Rev. Mod. Phys. **81**, 1551 (2009).
- [28] P. A. Lee, N. Nagaosa, and X.-G. Wen, Rev. Mod. Phys. **78**, 17 (2006).
- [29] M. Sigrist and K. Ueda, Rev. Mod. Phys. **63**, 239 (1991).
- [30] T.-L. Ho, Phys. Rev. Lett. **75**, 1186 (1995).
- [31] N. Read and E. Rezayi, Phys. Rev. B **54**, 16864 (1996).
- [32] K. Takada, H. Sakurai, E. Takayama-Muromachi, F. Izumi, R. A. Dilanian, and T. Sasaki, Nature **422**, 53 (2003).
- [33] T. Fujimoto, G.-q. Zheng, Y. Kitaoka, R. L. Meng, J. Cmaidalka, and C. W. Chu, Phys. Rev. Lett. **92**, 047004 (2004).
- [34] G.-q. Zheng, K. Matano, D. P. Chen, and C. T. Lin, Phys. Rev. B **73**, 180503 (2006).
- [35] S. Katsura, T. Ide, and T. Morita, Journal of Statistical Physics **42**, 381 (1986), 10.1007/BF01127717.
- [36] T. Jolicœur, E. Dagotto, E. Gagliano, and S. Bacci, Phys. Rev. B **42**, 4800 (1990).
- [37] Villain, J., Bidaux, R., Carton, J.-P., and Conte, R., J. Phys. France **41**, 1263 (1980).
- [38] C. L. Henley, Phys. Rev. Lett. **62**, 2056 (1989).
- [39] A. V. Chubukov and T. Jolicœur, Phys. Rev. B **46**, 11137 (1992).
- [40] E. Berg, C.-C. Chen, and S. A. Kivelson, Phys. Rev. Lett. **100**, 027003 (2008).
- [41] E. Rastelli, L. Reatto, and A. Tassi, Journal of Physics C: Solid State Physics **19**, 6623 (1986).
- [42] J. Ferrer, Phys. Rev. B **47**, 8769 (1993).
- [43] P. Sindzingre, L. Seabra, N. Shannon, and T. Momoi, Journal of Physics: Conference Series **145**, 012048 (2009).
- [44] P. Sindzingre, N. Shannon, and T. Momoi, Journal of Physics: Conference Series **200**, 022058 (2010).
- [45] L. Balents, Nature **464**, 199 (2010).
- [46] S. Sachdev, Phys. Rev. B **45**, 12377 (1992).
- [47] F. Wang and A. Vishwanath, Phys. Rev. B **74**, 174423 (2006).
- [48] A. V. Chubukov, S. Sachdev, and T. Senthil, Nuclear Physics B **426**, 601 (1994).
- [49] X.-G. Wen, Phys. Rev. B **65**, 165113 (2002).
- [50] This is true as long as $\vec{v}_x^{\mathcal{C}} \times \vec{v}_y^{\mathcal{C}} \neq 0$, which is always satisfied by a nodal Dirac point. (k_1, k_2) can be viewed as the two-dimensional momenta in a another coordinate system.
- [51] We verified that 2nd NN hopping amplitudes will not alter the spinon band minima and thus the magnetic ordering pattern upon spinon condensation.